Circulation Research

ORIGINAL RESEARCH

Prdm16 Supports Arterial Flow Recovery by Maintaining Endothelial Function

Sander Craps, Jore Van Wauwe, Sofie De Moudt, Dorien De Munck, Arthur J.A. Leloup, Bram Boeckx, Tim Vervliet, Wouter Dheedene, Nathan Criem, Carla Geeroms, Elizabeth A.V. Jones, An Zwijsen, Diether Lambrechts, Paul Fransen, Manu Beerens,* Aernout Luttun*

RATIONALE: Understanding the mechanisms that regulate arterial flow recovery is important to design treatment options for peripheral artery disease patients ineligible for invasive revascularization. Transcriptional orchestrators of this recovery process represent an appealing target for treatment design. We previously identified Prdm (positive regulatory domain-containing protein) 16 as an arterial-specific endothelial transcription factor but its in vivo role in arteries remains completely unknown.

OBJECTIVE: To unravel the role of Prdm16 in arteries under physiological and pathological conditions, more specifically during peripheral artery disease.

METHODS AND RESULTS: Within the vasculature, Prdm16 expression was strictly confined to arterial endothelial and smooth muscle cells. Heterozygous loss of *Prdm16* caused a modest reduction of the inner arterial diameter and smooth muscle cell coating without compromising vasomotor function. Upon femoral artery ligation, *Prdm16*$^{+/-}$ mice featured significantly impaired flow recovery to ischemic limbs. This impairment was recapitulated in mice with a *Prdm16* deletion specifically in endothelial cells (*EC-Prdm16*$^{-/-}$) but not smooth muscle cells. Structural collateral remodeling was normal in both *Prdm16*$^{+/-}$ and *EC-Prdm16*$^{-/-}$ mice, but significant endothelial dysfunction postligation was present in *EC-Prdm16*$^{-/-}$ mice as evidenced by impaired endothelial-dependent relaxation. Upon ligation, endothelial *Prdm16* deficiency altered the expression of genes encoding endothelial cell function regulators, many related to nitric oxide bioavailability and Ca^{2+} homeostasis. Accordingly, Prdm16 overexpression in cultured endothelial cells affected both total cellular Ca^{2+} levels and store-operated Ca^{2+} entry.

CONCLUSIONS: We showed that Prdm16 is indispensable for arterial flow recovery under pathological challenge not because it affects structural remodeling but due to its role in maintaining endothelial function. It, therefore, represents an appealing target for designing novel therapeutic strategies for no-option patients with peripheral artery disease.

GRAPHIC ABSTRACT: A graphic abstract is available for this article.

Key Words: arteries ■ endothelium ■ homeostasis ■ ischemia ■ transcription factor ■ vasodilation

Editorial, see p 78 | Meet the First Author, see p 4

The blood vascular system has a dual structure composed of an arterial and venous arm.[1] The former provides oxygenated blood to tissues, and the latter recirculates deoxygenated blood to heart and lungs for reoxygenation. These opposite functions are mirrored by distinct molecular and morphological signatures in endothelial cells (ECs) lining the inside of arteries and veins. The existence of arterial-specific diseases (eg, atherosclerosis) is a likely consequence of these distinct features.[2] Understanding the mechanisms determining the arterial EC signature is equally important for development of treatments tailored towards improving

Correspondence to: Aernout Luttun, PhD, Cardiovascular Sciences Department/ Center for Molecular and Vascular Biology, Endothelial Cell Biology Unit, KU Leuven, Campus Gasthuisberg, Onderwijs&Navorsing 1, Herestraat 49, Box 911, B-3000 Leuven, Belgium. Email aernout.luttun@kuleuven.be or Manu Beerens, PhD, Brigham and Women's Hospital, Harvard Medical School, Boston, MA. Email mbeerens@bwh.harvard.edu

*M. Beerens and A. Luttun contributed equally.

The Data Supplement is available with this article at https://www.ahajournals.org/doi/suppl/10.1161/CIRCRESAHA.120.318501.

For Sources of Funding and Disclosures, see page 76.

ORIGINAL RESEARCH

Novelty and Significance

What Is Known?

- Endothelial cells (ECs) in arteries have a distinct expression pattern including transcription factors.
- During peripheral artery disease (PAD), the impaired arterial blood supply triggers a rescue response that is orchestrated by transcription factors.
- Prdm (positive regulatory domain-containing protein) 16 is a transcription factor mostly known for its role in the skeletal, adipose, hematopoietic, and nervous systems.

What New Information Does This Article Contribute?

- Prdm16 is a general marker of ECs and smooth muscle cells in the arterial but not venous arm of the adult vascular system.
- Prdm16 in arterial ECs but not smooth muscle cells (SMCs) is indispensable for normal arterial blood flow recovery during PAD.
- Prdm16 supports normal arterial blood flow recovery not by mediating the structural collateral arterial remodeling response but rather by preserving arterial endothelial function.

Arterial ECs have a distinct profile that makes them vulnerable to artery-restricted diseases like PAD. Upon PAD, limb blood flow is impaired which causes damage sometimes necessitating amputation. The impaired blood flow triggers a rescue mechanism driven by transcription factors during which flow is redirected through collateral arteries that thereby feature structural changes. Identifying these transcription factors and revealing their mode of action is crucial for designing novel strategies to improve arterial blood flow and avoid amputation in PAD patients. Here, we found that Prdm16 is a transcription factor highly expressed in arterial ECs and SMCs. Through its expression in arterial ECs, Prdm16 rescued arterial blood flow upon PAD. Surprisingly, the mechanism of action was not related to governing the structural collateral remodeling process but rather to preserving endothelial function. Unlike most research in the PAD field, the present study establishes that supporting structural collateral remodeling is not the only important action to guarantee normal arterial blood flow recovery as the latter equally relies on preserving EC functionality. We identified Prdm16 as a key promoter of arterial EC function during PAD. Hence, Prdm16 represents an interesting target to design novel PAD treatment strategies that ideally should combine structural and functional rescue.

Nonstandard Abbreviations and Acronyms

DA	descending aorta
DEG	differentially expressed gene
Dll4	delta-like ligand 4
EC	endothelial cell
Ehd2	EH domain-containing 2
eNOS	endothelial NO synthase
ER	endoplasmic reticulum
FA	femoral artery
Fbln5	fibulin 5
FGF	fibroblast growth factor
HLI	hindlimb ischemia
Msx	muscle segment homeobox
Nox	NADPH-oxidase
PAD	peripheral artery disease
Prdm	positive regulatory domain-containing protein
SMA	smooth muscle actin
SMC	smooth muscle cell
Timp	tissue inhibitor of metalloproteinases
VEGF	vascular endothelial growth factor
WT	wild-type

growth of arteries and preserving their specific functions during ischemic diseases caused by insufficient arterial blood supply.

Limb ischemia, known as peripheral artery disease (PAD), affects 200 million people worldwide, and this number will further increase in the aging population.[3] Current revascularization strategies are mainly invasive procedures for which many PAD patients are ineligible due to the presence of risk factors or multiple-vessel occlusion.[4] Although noninvasive alternatives, for example, administration of general angiogenic growth factors like VEGF (vascular endothelial growth factor) and FGF (fibroblast growth factor) have been tested for no-option patients, these have shown limited success,[5] potentially due to lack of specificity towards an arterial response. Hence, the advent of more tailored molecular therapies is eagerly awaited. Designing such therapies requires a thorough mechanistic understanding of the arterial flow recovery process upon arterial obstruction.

To cope with such an obstruction, the vascular system has a collateral reserve network in which collateral arteries connect 2 nurturing arteries such that flow can be redirected. Sudden exposure to flow imposes shear stress on collateral ECs which triggers structural and functional changes, that is, luminal expansion and acquisition of a

thicker smooth muscle cell (SMC) coat.[6] This remodeling process is known as adaptive arteriogenesis and converges on transcription factors. Msx (muscle segment homeobox) 1 is part of a mechanosensing pathway that fuels collateral arterial growth. It induces a proinflammatory state in collateral ECs, enabling them to recruit monocytes to initiate collateral expansion.[7] In addition to shear stress-driven collateral growth proximal to the obstruction, hypoxia triggers capillary growth more distally. This angiogenic response is also mediated through transcription factors (eg, TFEB [trancription factor-EB]).[8]

Inspired by the finding that Msx1 triggered structural collateral growth during PAD,[7] we sought to determine whether other transcription factors from our previously established arterial EC signature were also involved.[9] Prdm (positive regulatory domain-containing protein) 16 emerged as a likely candidate as it was the most differentially expressed transcription factor with an unknown role in arteries in vivo.[9] Prdm16 is part of a family of 17 members that are involved in a spectrum of biological processes including cell fate decision making.[10] Although initially identified as an oncogene in myelodysplastic syndrome and acute myeloid leukemia,[11] Prdm16 is currently mostly known for its roles in brown/beige adipose tissue fate decision,[10,12] craniofacial development,[13] hematopoietic/neuronal stem cell maintenance, and homeostasis[14,15] and in the context of certain cardiomyopathies.[16] Accordingly, Prdm16 expression has been documented in brown and beige adipose tissue, the skeletal, hematopoietic, and nervous systems and the heart.[10,11,13–15] Constitutive homozygous deficiency of *Prdm16* in mice causes respiratory failure and perinatal death.[13] Recently, Prdm16 expression was reported in retinal arterioles,[17] yet, a detailed analysis of its expression and role in the adult arterial system, more specifically during adaptive arteriogenesis, remains unexplored.

METHODS

Extended methods and a Major Resources Table (Table I in the Data Supplement) are provided in the Data Supplement.

Data Availability

The authors declare that the majority of supporting data are presented within this article and in the Data Supplement. Data not directly presented are available from the corresponding author upon reasonable request. Single-cell RNA sequencing data have been deposited in the ArrayExpress database at EMBL-EBI (www.ebi.ac.uk/arrayexpress; accession number E-MTAB-9703).

Mouse Strains and Cell Type–Specific Prdm16 Deletion

Animal experiments were approved by the KU Leuven Ethics Committee on Animal Use. Three mouse lines were used: ubiquitous constitutive *Prdm16* knockout mice (*Prdm16*$^{Gt(OST67423)Lex}$; or *Prdm16*$^{+/-}$)[13]; EC-specific *Prdm16* knockout mice (*Cdh5-Cre*^{ERT2}*;Prdm16*$^{fl/fl}$; or *EC-Prdm16*$^{-/-}$) generated by intercrossing the *Cdh5-Cre*^{ERT2} driver line[18] with *Prdm16*$^{fl/fl}$ mice[19]; mice with *Prdm16* deficiency in SMCs (*Sm22α-Cre;Prdm16*$^{fl/fl}$; or *SMC-Prdm16*$^{-/-}$) generated by crossing the *Sm22α-Cre* driver line[20] with *Prdm16*$^{fl/fl}$ mice. EC-specific *Prdm16* deletion was induced by tamoxifen (4 intragastric injections on postnatal day 1 to 4 for long-term deletion or, for short-term deletion, 5 daily injections in week 10, starting 14 days before hindlimb ischemia (HLI) induction). Tamoxifen-induced deletion efficacy was ≈80% and Prdm16 loss in collaterals was restricted to ECs or SMCs in *EC-Prdm16*$^{-/-}$ and *SMC-Prdm16*$^{-/-}$ mice, respectively (Figure I in the Data Supplement).

Prdm16 Expression Analysis

Prdm16 expression was examined by X-gal 5-bromo-4-chloro-3-indolyl-D-galactopyranoside (X-gal) staining (taking advantage of the presence of a gene-trap cassette in the *Prdm16* locus encoding β-galactosidase in *Prdm16*$^{+/-}$ mice)[13] or by an in-house optimized immunofluorescence staining.

Structural, Biomechanical, and Blood Pressure Measurements

Inner diameter and SMC cross-sectional area of descending aorta (DA) and femoral artery (FA) were measured in cross-sections of adult *Prdm16*$^{+/+}$ and *Prdm16*$^{+/-}$ mice. Biomechanical measurements were obtained by mounting DA segments in a Rodent Oscillatory Tension Set-Up to Study Arterial Compliance.[21] Blood pressure was determined via noninvasive tail-cuff measurements on a CODA system (Kent Scientific).

HLI Induction and Follow-Up

HLI studies were performed in 8- to 12-week old *Prdm16*$^{+/-}$, *EC-Prdm16*$^{-/-}$, *SMC-Prdm16*$^{-/-}$ mice and their wild-type (WT) littermates by FA ligation.[7] Reperfusion recovery was monitored by laser doppler imaging (Lisca, PIMII), and necrosis was assessed by an in-house developed necrosis score. At day 3 or day 21 postligation, adductor or gastrocnemius muscles were dissected out and processed for histology, RNA, or protein extraction. Gene expression was quantified by quantitative real-time polymerase chain reaction as described online using primer sets listed in Table II in the Data Supplement. Protein quantification was performed by Western blotting, as described online. Fibrosis/fibroadipose tissue[22] in day 21 postligation gastrocnemius muscles was investigated on Sirius red-stained cross-sections. Collateral remodeling in the adductor region was evaluated by studying inflammatory cell recruitment around growing collaterals at day 3 postligation on Cd45- or Cd68-αSMA (smooth muscle actin) double-stained cross-sections and by determining luminal and medial expansion at day 21 postligation on Cd31-αSMA double-stained cross-sections. To determine capillary density in the gastrocnemius muscle, an identical Cd31/αSMA staining was used. Morphometry was performed by a blinded investigator.

Nano–Computed Tomography

Prdm16$^{+/-}$ and *Prdm16*$^{+/+}$ littermates were subjected to FA ligation and perfused 7 days later with barium sulfate/gelatin. After overnight solidification, limbs were dissected out and scanned with a Phoenix Nanotom M, and scans were optimized

during three-dimensional reconstruction (Datos|x, Waygate Technologies). Images were analyzed as described online.

Organ Bath and Myograph Measurements

DA and FA segments of *Prdm16*$^{+/-}$ or long-term *EC-Prdm16*$^{-/-}$ mice and their corresponding WT littermates were dissected out and mounted in an organ bath or on a myograph (DMT, 610M), respectively.[23,24] Active contractions and relaxations were monitored during cumulative dose exposure to phenylephrine (contraction), acetylcholine (EC-dependent relaxation), or diethylamine NONOate (EC-independent relaxation). To study vasomotor function upon HLI, right FA segments downstream of the ligation site of *Prdm16*$^{+/-}$ or long-term *EC-Prdm16*$^{-/-}$ mice, and their corresponding WT littermates were isolated and mounted on a myograph day 3 postligation. FA segments of the unligated left side served as control. For *EC-Prdm16*$^{-/-}$ and WT littermates, DA vasomotor function was recorded from the same mice.

Single-Cell RNA Sequencing

On day 3 postligation, FA segments downstream of the ligation and corresponding segments on the unligated side from *EC-Prdm16*$^{-/-}$ or *EC-Prdm16*$^{+/+}$ littermates (n=4 each) were dissected out and collected on ice. FA segments were pooled per sample type (ligated and unligated, for both *EC-Prdm16*$^{-/-}$ and *EC-Prdm16*$^{+/+}$), converted into single-cell suspensions, and barcoded libraries were prepared using kits from 10X Genomics and sequenced on an Illumina Nextseq and NovaSeq6000 as described online. Raw data processing, quality control (Figure II in the Data Supplement), comparative analysis of *Cd45*$^{+}$ (*Ptprc*$^{+}$) clusters, and differential expression/functional annotation analyses of the arterial EC cluster was performed as described online using Cell Ranger, Harmony, and MAST software packages/algorithms.[25–27]

Lentiviral Transduction and Ca^{2+} Measurements

A lentivirus overexpressing full-length mouse Prdm16 (clone ID 6409778; Thermo Scientific Molecular Biology) was used.[9] Human umbilical vein ECs (generated after obtaining informed consent from donors)[9] were transduced and after 6 days, harvested and seeded for Ca^{2+} measurements. As control, cells were transduced with a Cherry-expressing lentivirus. Human umbilical vein ECs were loaded with Fura-2AM (Fura-2 acetoxymethyl) and total cellular and endoplasmic reticulum (ER) Ca^{2+} content and store-operated Ca^{2+} entry were measured 24 hours later as described online.

Statistics

Continuous data are presented as mean±SEM. Detailed information on statistics is provided in the Data Supplement (Table III in the Data Supplement).

RESULTS

Prdm16 Universally Marks Adult Arteries

From comparative profiling of human umbilical cord ECs, *PRDM16* emerged as an arterial EC-enriched transcription factor.[9] This expression pattern was conserved in adult mice, as Prdm16 was only detectable in arteries and not veins, with strong expression in both ECs and SMCs. This arterial-exclusive expression was present in the intima and media of multiple adult blood vessel types with strong expression in the carotid artery, thoracic aorta, and FA, the former 2 representing elastic conduit arteries, the third one being a smaller caliber muscular artery (Figure 1A through 1F). Similar observations were made in other arteriovenous pairs (Figure IIIA through IIID in the Data Supplement). Whole-mount staining of the retina revealed that arterial expression was retained down to the arteriolar level (Figure 1G), in accordance with a previous study.[17] Next to physiological conditions, Prdm16 expression was also prominent in ECs and SMCs of collateral arteries following HLI induction (Figure 1H). Compared with the unligated side, Prdm16 expression in collateral ECs and SMCs was relatively stable during the first 3 days postligation, then subsequently declined followed by a slow recovery from day 7 onwards (Figure IIIE and IIIF in the Data Supplement). Thus, Prdm16 universally marked ECs and SMCs of arteries and not veins, independent of anatomic location, vessel caliber, artery type, or health status.

Ubiquitous Heterozygous *Prdm16* Deficiency Does Not Affect Arterial Vasomotor Function

Next, we questioned whether the arterial-restricted expression pattern of Prdm16 reflected a functional role in adult arteries under physiological conditions. Although homozygous *Prdm16* deficiency causes respiratory failure and death around birth,[13] heterozygous *Prdm16* mice were viable and fertile. DA and FA dimensions were slightly smaller in *Prdm16*$^{+/-}$ *versus* *Prdm16*$^{+/+}$ mice (Figure 2A through 2C). SMC cross-sectional area was significantly decreased in the FA and showed a trend towards decrease in the DA in *Prdm16*$^{+/-}$ mice (Figure 2D through 2F). Despite reduced arterial dimensions, baseline arterial vasomotor function was normal, as evidenced by identical blood pressure (not shown) and similar maximal contraction and EC-dependent or EC-independent relaxation in the DA and FA of *Prdm16*$^{+/-}$ and *Prdm16*$^{+/+}$ littermates (Figure 2G through 2O). Further examinations showed normal biomechanical properties of *Prdm16*$^{+/-}$ DA segments at physiological stretch frequency and pressure (Figure IV in the Data Supplement). Thus, *Prdm16* heterozygous deficiency did not affect baseline arterial vasomotor function or biomechanics.

Ubiquitous or EC-Specific *Prdm16* Deficiency Impairs Arterial Flow Recovery Upon HLI

To test whether Prdm16 had a role in arteries during PAD, FAs of *Prdm16*$^{+/-}$ and *Prdm16*$^{+/+}$ littermates were ligated to trigger adaptive arteriogenesis. *Prdm16*$^{+/+}$

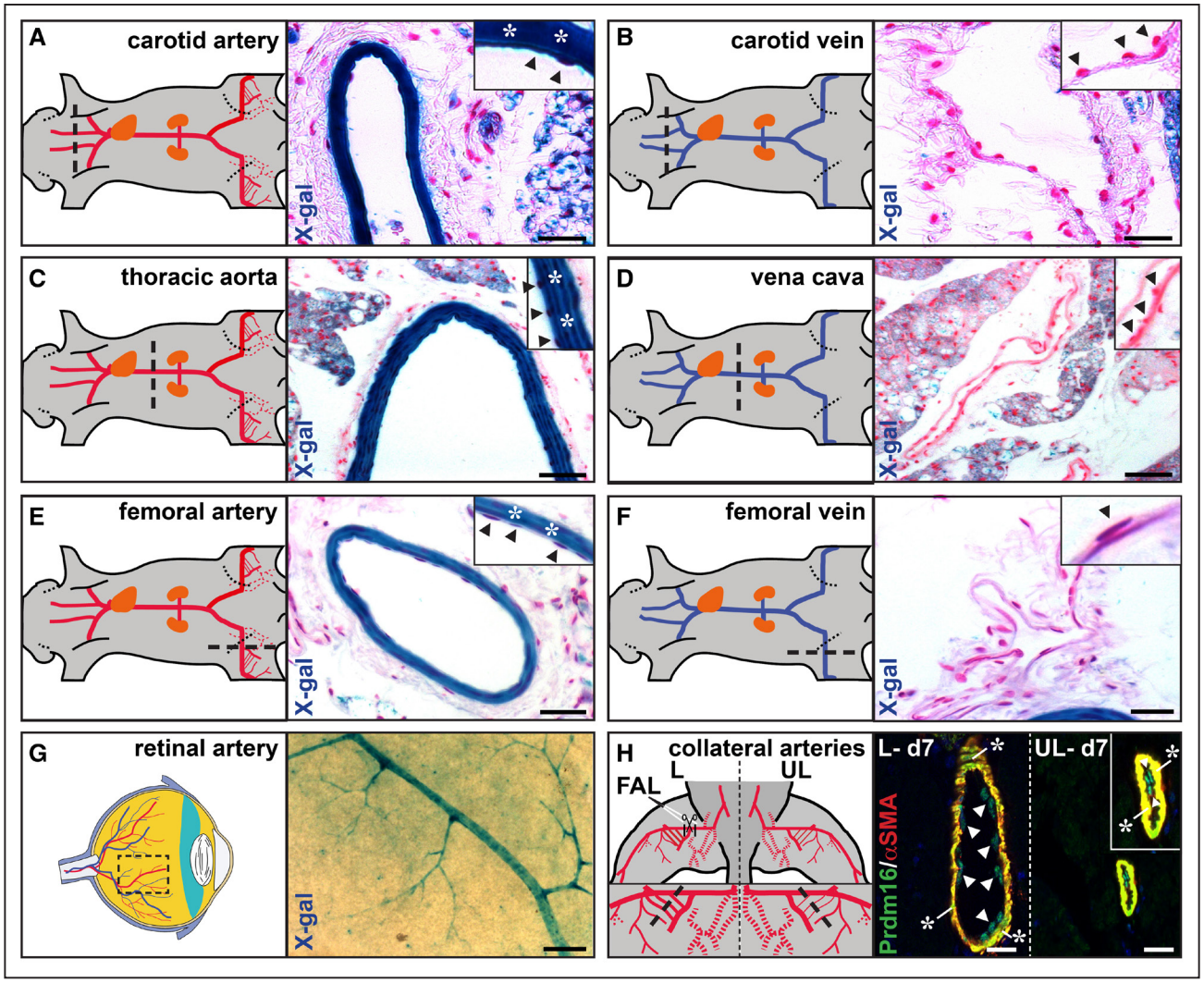

Figure 1. Prdm (positive regulatory domain-containing protein) 16 is a universal arterial marker in health and disease.
A–**F**, X-gal (5-bromo-4-chloro-3-indolyl–D-galactopyranoside) staining on cross-sections of adult *Prdm16*$^{+/-}$ arteriovenous pairs. Arteries are shown in (**A**, **C**, and **E**), venous counterparts in (**B**, **D**, and **F**). **G**, Whole-mount X-gal staining on a flat-mounted retina of a *Prdm16*$^{+/-}$ adult mouse. **H**, Immunofluorescence staining for Prdm16 (green) and αSMA (smooth muscle actin; red) on adductor sections of the unligated (UL) and ligated (L) side 7 d after femoral artery ligation (FAL). Arrowheads and asterisks indicate endothelial and smooth muscle cells, respectively, in **A**–**F**, and **H.** Black dashed lines in **A**–**F**, and **H** and dashed box in **G** show location of the cross-section or whole-mount staining. Scale bars: 50 μm in **A**–**F**, 25 μm in **G**, and 10 μm in **H**.

mice had spontaneous arterial flow recovery to >80% at day 21, whereas recovery was impaired from day 7 onwards in *Prdm16*$^{+/-}$ mice (Figure 3A and 3B; Figure VA and VB in the Data Supplement). Accordingly, *Prdm16*$^{+/-}$ mice had more tissue necrosis, fibrosis, and fibro-adipose tissue in their gastrocnemius muscles than *Prdm16*$^{+/+}$ littermates (Figure 3C and 3D; Figure VC through VE in the Data Supplement). Because Prdm16 was expressed in both EC and SMC compartments, we investigated which cell type was mainly responsible for the defective flow recovery by inducing HLI in mice with *Prdm16* deficiency in ECs or SMCs using Cre-mediated excision driven by the tamoxifen-inducible *Cdh5* or the constitutive *Sm22α* promoter, respectively. Long-term (ie, from birth onwards) *Prdm16* deficiency in ECs caused a significant impairment in arterial flow recovery, compared with their corresponding WT littermates, which was accompanied by worsened tissue necrosis, more fibrosis, and fibro-adipose tissue in the gastrocnemius muscle (Figure 3E through 3H; Figure VF through VJ in the Data Supplement). When shortening the duration of *Prdm16* deficiency in ECs by starting tamoxifen administration only 14 days before HLI induction, the impairment in flow recovery was shifted towards a later time-point (Figure 3I and 3J; Figure VK and VL in the Data Supplement) and follow-up until 6 weeks after HLI induction revealed that this impairment did not resolve later on (not shown). This less severe recovery deficit also correlated with lower scores for necrosis, fibrosis, and fibro-adipose tissue (Figure 3K and 3L; Figure VM through VO in the Data Supplement). In contrast, constitutive *Prdm16* loss in SMCs did not impair arterial flow recovery (Figure 3M

ORIGINAL RESEARCH

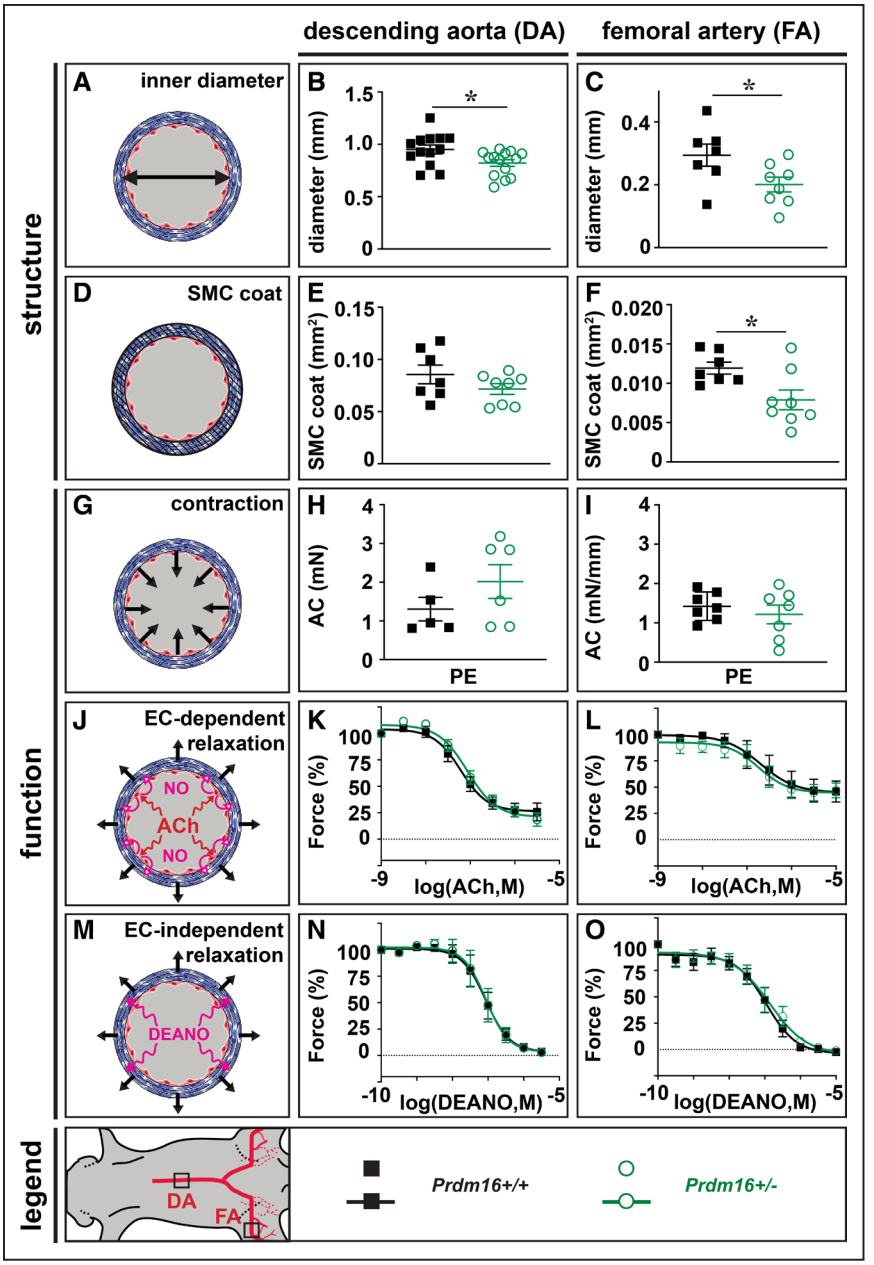

Figure 2. Ubiquitous heterozygous *Prdm (positive regulatory domain-containing protein) 16* deficiency slightly affects arterial geometry but not vasomotor function.
A–**C**, Schematic representation (**A**) and quantification of descending aorta (DA; **B**) and femoral artery (FA; **C**) diameter of *Prdm16*$^{+/+}$ (n=13 for DA; n=7 for FA) and *Prdm16*$^{+/-}$ (n=14 for DA; n=8 for FA) mice. **D**–**F**, Schematic representation (**D**) and quantification of DA (**E**) and FA (**F**) smooth muscle cell (SMC) cross-sectional area of *Prdm16*$^{+/+}$ (n=7 for DA and FA) and *Prdm16*$^{+/-}$ (n=8 for DA and FA) mice. **G**–**I**, Schematic representation (**G**) and quantification of the phenylephrine (PE)-induced absolute contraction (AC) in DA (**H**) and FA (**I**) of *Prdm16*$^{+/+}$ (n=5 for DA; n=7 for FA) and *Prdm16*$^{+/-}$ (n=6 for DA; n=7 for FA) mice (concentration PE: 3×10^{-6} mol/L for DA and FA). **J**–**L**, Schematic representation (**J**) and quantification of relative acetylcholine (ACh)-mediated relaxation of DA (**K**) and FA (**L**) from *Prdm16*$^{+/+}$ (n=6 for DA; n=7 for FA) and *Prdm16*$^{+/-}$ (n=5 for DA; n=7 for FA) mice. **M**–**O**, Schematic representation (**M**) and quantification of relative diethylamine NONOate (DEANO)–mediated relaxation of DA (**N**) and FA (**O**) from *Prdm16*$^{+/+}$ (n=6 for DA; n=7 for FA) and *Prdm16*$^{+/-}$ (n=6 for DA; n=7 for FA) mice. Data represent mean±SEM. *$P<0.05$: vs corresponding control (Table III in the Data Supplement). EC indicates endothelial cell, and M in (K,L,N,O), molar.

and 3N; Figure VP and VQ in the Data Supplement). Accordingly, there was no alteration in necrosis, fibrosis, or fibro-adipose tissue in *SMC-Prdm16*$^{-/-}$ *versus SMC-Prdm16*$^{+/+}$ gastrocnemius muscles (Figure 3O and 3P; Figure VR through VT in the Data Supplement). Thus, *Prdm16* deficiency in ECs but not SMCs had a detrimental time-dependent effect on arterial flow recovery.

Ubiquitous or EC-Specific *Prdm16* Deficiency Does Not Impair Vessel Remodeling Upon HLI

Structural vascular remodeling during adaptive arteriogenesis is initiated by inflammatory cell recruitment towards the endothelium of collaterals which primes them for luminal and medial expansion.[7,28] Recruitment of Cd45^{+} cells around growing collaterals at the ligated side at day 3 postligation in the adductor region was unaltered in *Prdm16*$^{+/-}$ and long-term *EC-Prdm16*$^{-/-}$ mice compared with their corresponding WT littermates (Figure 4A through 4C; Figure VIA through VID in the Data Supplement). Accordingly, the increase in inner diameter and SMC cross-sectional area of the remodeled collaterals was not affected by ubiquitous or EC-restricted *Prdm16* deficiency (Figure 4D through 4I; Figure VIE through VIH in the Data Supplement). Analysis of the day 3 Cd45^{+} cell infiltrate around *EC-Prdm16*$^{-/-}$ arteries at single-cell resolution revealed 4 *Cd45*$^{+}$ (*Ptprc*$^{+}$) cell types among the 14 annotated clusters, that is, *Cd68*$^{+}$ monocyte/macrophages, *Ly6g*$^{+}$ monocyte/neutrophils, *Cd3*$^{+}$ T, and *Cd79a*$^{+}$ B lymphocytes (Figure VIIA through VIID in the Data Supplement). There were no major genotypic differences in extent or composition of the lymphoid/myeloid cell groups,

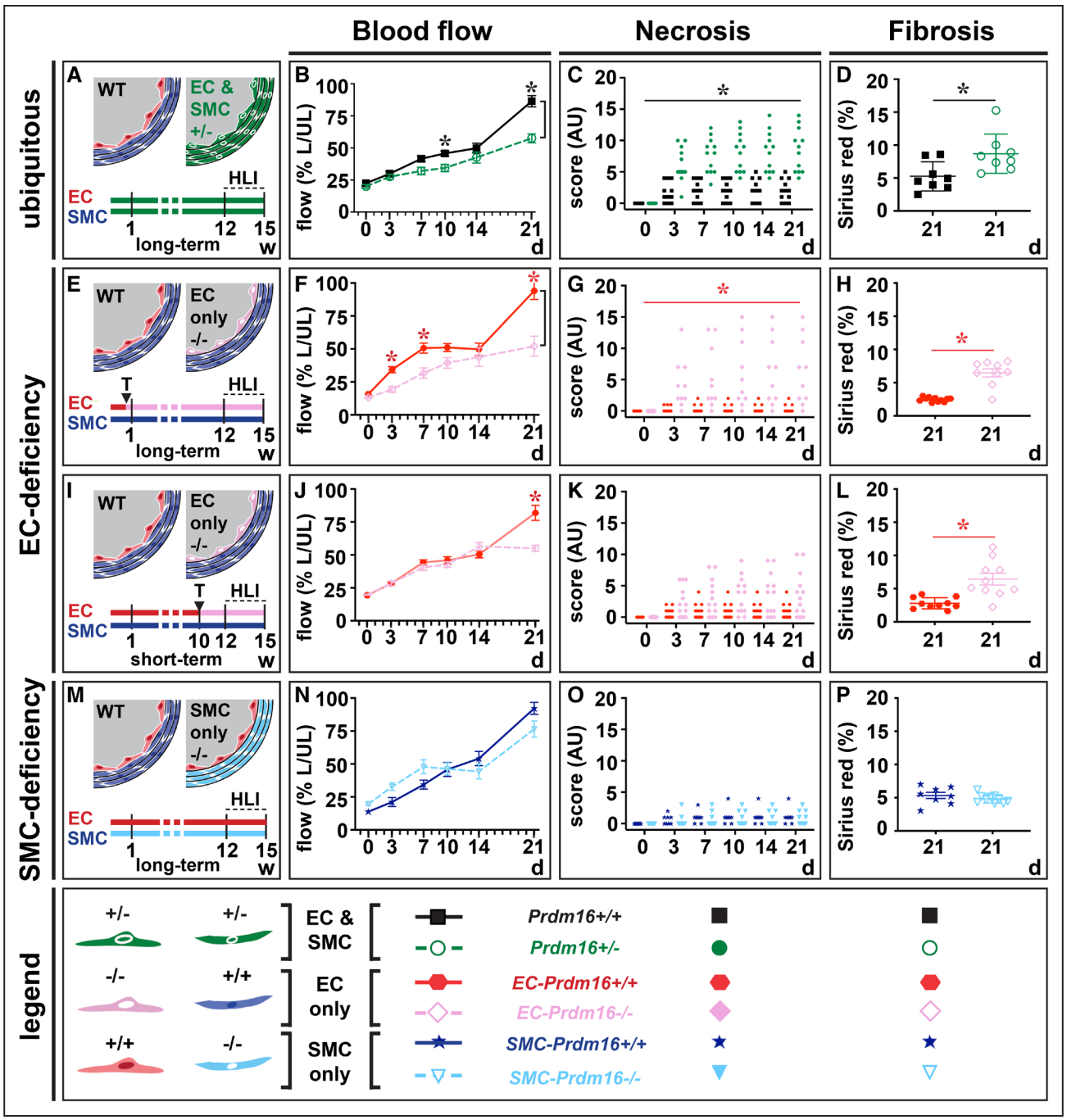

Figure 3. Ubiquitous or endothelial cell (EC)–specific *Prdm (positive regulatory domain-containing protein) 16* deficiency impair flow recovery and boost necrosis and fibrosis upon hindlimb ischemia (HLI).
A–**D**, Schematic representation/time-line (**A**; w [weeks]; wild-type [WT]) and quantification of flow recovery (**B**; expressed as % of ligated [L] over unligated [UL]), d 21 necrosis (**C**; expressed in arbitrary units [AU]) and d 21 fibrosis scores (**D**) in *Prdm16*$^{+/+}$ (n=8–12) or *Prdm16*$^{+/-}$ (n=8–12) mice after HLI induction. **E**–**H**, Schematic representation/time-line (**E**; T: tamoxifen) and quantification of flow recovery (**F**; expressed as % of L over UL), d 21 necrosis (**G**; expressed in AU), and d 21 fibrosis scores (**H**) in long-term *EC-Prdm16*$^{+/+}$ (n=11–12) or *EC-Prdm16*$^{-/-}$ (n=9–10) mice after HLI induction. **I**–**L**, Schematic representation/time-line (**I**) and quantification of flow recovery (**J**; expressed as % of L over UL), d 21 necrosis (**K**; expressed in AU) and d 21 fibrosis scores (**L**) in short-term *EC-Prdm16*$^{+/+}$ (n=10–16) or *EC-Prdm16*$^{-/-}$ (n=10–13) mice after HLI induction. **M**–**P**, Schematic representation/time-line (**M**) and quantification of flow recovery (**N**; expressed as % of L over UL), d 21 necrosis (**O**; expressed in AU), and d 21 fibrosis scores (**P**) in smooth muscle cell (*SMC*)-*Prdm16*$^{+/+}$ (n=8) or *SMC-Prdm16*$^{-/-}$ (n=10) mice after HLI induction. Data in **B**, **D**, **F**, **H**, **J**, **L**, **N**, and **P** represent mean±SEM. *P<0.05: vs corresponding control (Table III in the Data Supplement).

and the comparable Cd68^{+} monocyte/macrophage recruitment around *EC-Prdm16*$^{-/-}$ and *EC-Prdm16*$^{+/+}$ collaterals was confirmed by immunofluorescence staining (Figure VIIE through VIIJ in the Data Supplement). The lack of a remodeling deficit in *Prdm16*$^{+/-}$ adductors was confirmed by 3-dimensional reconstruction of the vessel

ORIGINAL RESEARCH

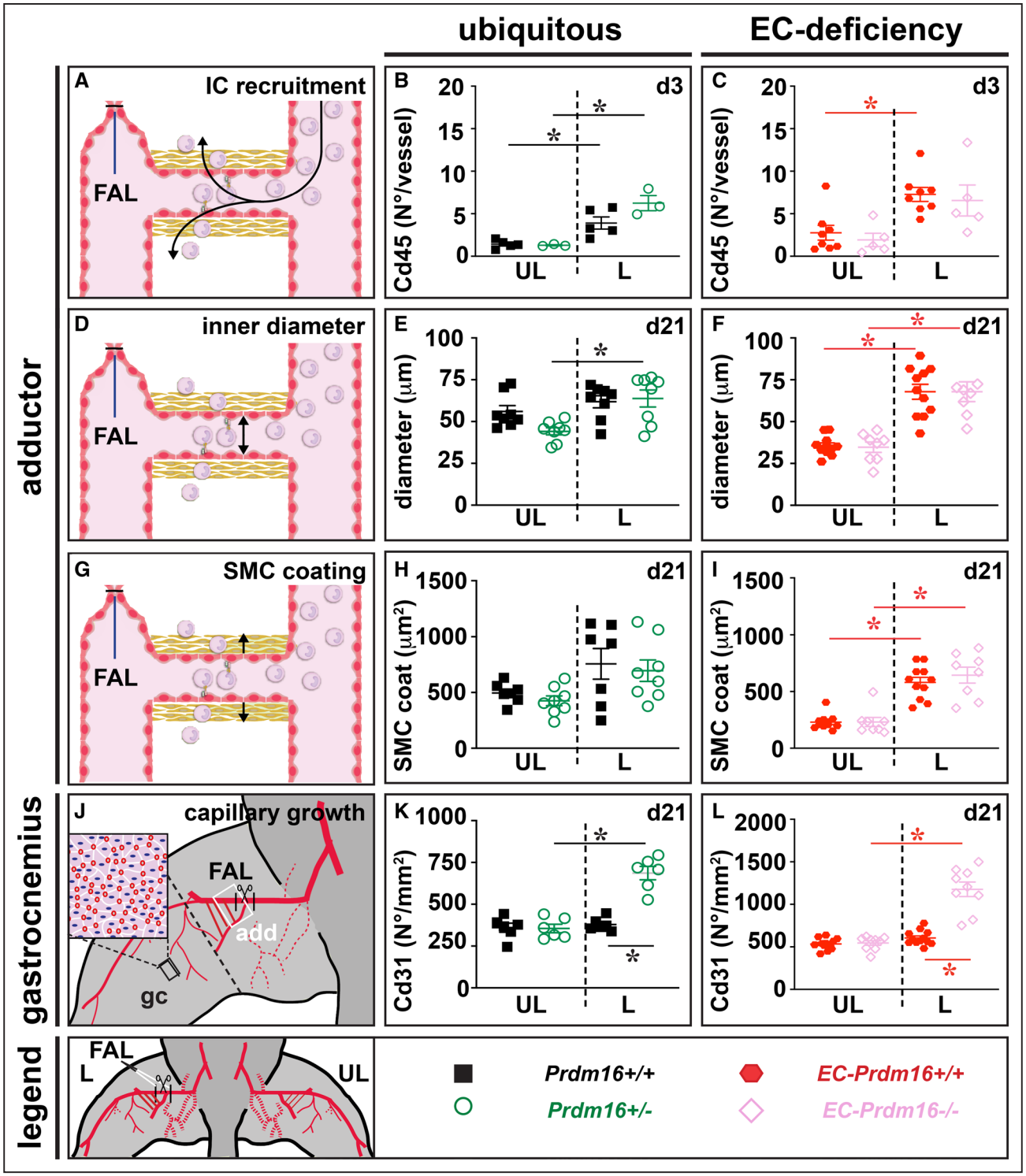

Figure 4. Ubiquitous or endothelial cell (EC)–specific *Prdm (positive regulatory domain-containing protein) 16* deficiency do not affect structural vascular remodeling upon hindlimb ischemia.

A–**C**, Schematic representation (**A**) and quantification of Cd45$^+$ inflammatory cell (IC) recruitment around expanding collaterals in the adductor region of the ligated (L) and unligated (UL) side at 3 d after femoral artery ligation (FAL) in *Prdm16*$^{+/+}$ (n=5) or *Prdm16*$^{+/-}$ (n=3) mice (**B**) and long-term *EC-Prdm16*$^{+/+}$ (n=8) or *EC-Prdm16*$^{-/-}$ (n=5) mice (**C**). **D**–**F**, Schematic representation (**D**) and quantification of collateral inner diameter at d 21 after FAL in *Prdm16*$^{+/+}$ (n=8) or *Prdm16*$^{+/-}$ (n=8) mice (**E**) and long-term *EC-Prdm16*$^{+/+}$ (n=11) or *EC-Prdm16*$^{-/-}$ (n=8) mice (**F**). **G**–**I**, Schematic representation (**G**) and quantification of smooth muscle cell (SMC)–coating (measured as cross-sectional medial area) of remodeled collateral arteries at d 21 after FAL in *Prdm16*$^{+/+}$ (n=7) or *Prdm16*$^{+/-}$ (n=8) mice (**H**) and long-term *EC-Prdm16*$^{+/+}$ (n=11) or *EC-Prdm16*$^{-/-}$ (n=8) mice (**I**). **J**–**L**, Schematic representation (**J**) and quantification of capillary density in gastrocnemius (gc; black box) muscle at d 21 after FAL in *Prdm16*$^{+/+}$ (n=6) or *Prdm16*$^{+/-}$ (n=6) mice (**K**) and long-term *EC-Prdm16*$^{+/+}$ (n=12) or *EC-Prdm16*$^{-/-}$ (n=9) mice (**L**). Data represent mean±SEM. *P<0.05: vs indicated condition (Table III in the Data Supplement). Adductor region (add) studied in **A**–**I** is indicated by a white box in **J**.

network by nano-computed tomography (CT), as evident from a comparable expansion of the total vascular volume or growth/remodeling of the collaterals (Figure VIII in the Data Supplement).

In addition to adaptive arteriogenesis in the adductor region, flow distribution to the downstream ischemic muscle can be improved by increasing capillary density in the gastrocnemius region.[8] Unlike in their *Prdm16*$^{+/+}$ littermates, Cd31^{+} capillary density in the gastrocnemius muscle of the ligated limb was significantly increased in *Prdm16*$^{+/-}$ and long-term *EC-Prdm16*$^{-/-}$ mice, likely representing a compensatory (but insufficient) response to aggravated ischemia driven by increased *Vegfa* levels (Figure 4J through 4L; Figure VII through VIL in the Data Supplement; not shown). Altogether, the deficit in flow recovery in *Prdm16*$^{+/-}$ and long-term *EC-Prdm16*$^{-/-}$ mice could not be explained by structural vascular remodeling impairment.

EC-Specific *Prdm16* Deficiency Causes Attenuated EC-Dependent Relaxation Upon HLI

To study vasomotor function upon HLI induction, FA segments downstream of the ligation site were isolated from *Prdm16*$^{+/-}$, long-term *EC-Prdm16*$^{-/-}$ and their corresponding WT littermates at day 3 postligation and mounted on a myograph. Phenylephrine-mediated contractions tended to be lower in FA segments of the ligated versus the unligated side but *Prdm16* deficiency did not affect contraction (Figure 5A through 5C). Likewise, EC-dependent relaxation in response to acetylcholine was altered in the FA segment of the ligated side, but this response was not impaired in *Prdm16*$^{+/-}$ compared with their *Prdm16*$^{+/+}$ littermates (Figure 5D and 5E). In contrast, HLI triggered a significantly lowered response to acetylcholine in long-term *EC-Prdm16*$^{-/-}$ compared with *EC-Prdm16*$^{+/+}$ FA segments on the ligated side (Figure 5D and 5F). Vice versa, EC-independent relaxation upon exposure to NO-donor diethylamine NONOate was not significantly affected by HLI or by *Prdm16* deficiency (Figure 5G through 5I). Vasomotor function of the FA at the unligated side (Figure 5C, 5F, and 5I) and the DA upstream of the ligation (Figure IX in the Data Supplement) was very similar between long-term *EC-Prdm16*$^{-/-}$ mice and their *EC-Prdm16*$^{+/+}$ littermates. Altogether, endothelial *Prdm16* deficiency resulted in early-onset EC dysfunction only when challenged by HLI.

Prdm16 in ECs Regulates Their Function Through Ca^{2+} and NO Homeostasis

To explore mechanisms of this early-onset EC dysfunction in an unbiased way, we performed in situ differential expression analysis in *EC-Prdm16*$^{-/-}$ and *EC-Prdm16*$^{+/+}$ littermates at day 3 postligation by single-cell RNA sequencing of FA segments from the ligated and unligated side. Cluster analysis revealed 14 cell populations, including *Sox17*$^{+}$ arterial ECs (Figure 6A and 6B; Figure VIIA through VIIC in the Data Supplement). To identify genes with altered expression specifically in arterial ECs by induction of HLI in a Prdm16-dependent or Prdm16-independent way, we performed a 2-step analysis (Figure 6C). First, we shortlisted (based on statistical significance, degree of differential expression, and percentage of cells featuring expression changes) the genes altered by FA ligation by comparing the ligated and unligated side for *EC-Prdm16*$^{+/+}$ and *EC-Prdm16*$^{-/-}$ separately. Next, we overlapped these shortlists to distinguish genes commonly regulated (type A genes) from those that were uniquely changed (type B genes) among genotypes. This revealed 218 type A and 398 type B genes, of which 217 were uniquely altered in *EC-Prdm16*$^{+/+}$ (type B1 genes) and 181 were exclusively changed in *EC-Prdm16*$^{-/-}$ mice (type B2 genes). We considered both type B1 and B2 genes to be potentially involved in the observed EC dysfunction (Figure 6C; Tables IV and V in the Data Supplement). We next performed functional annotation analysis on type B1 and B2 genes to identify and prioritize unique genotype-dependent processes known to be involved in EC function. Among prioritized functions related to type B1 genes, we identified gap junctions and endocrine and other factor-related Ca^{2+} reabsorption, whereas Ca^{2+} binding and multiple functional terms related to fat(ty acid) handling were found associated with type B2 genes (Figure 6D: Tables VI and VII in the Data Supplement).

Accordingly, an in-depth literature analysis on the 30 type B genes—the majority of which were downregulated upon ligation—associated with the prioritized functions revealed that as many as 50% of them related to Ca^{2+} handling (Figure 6E; Table VIII in the Data Supplement). Next, because the vascular relaxation deficit in *EC-Prdm16*$^{-/-}$ mice was no longer apparent after NO-donor supplementation, we hypothesized that changes in prioritized genes might reflect altered regulation of NO bioavailability. NO decrease can be caused by reduced levels/activity of eNOS (endothelial NO synthase) or by Nox (NADPH-oxidase)-induced eNOS uncoupling, the latter resulting in production of radical oxygen species rather than NO.[29] In support of this hypothesis, 33% of prioritized genes have a documented involvement in eNOS regulation/NO production, and 17% are known to be involved in redox status regulation (Figure 6E; Table VIII in the Data Supplement). Finally, ≈43% of the prioritized genes have been associated with the process of clathrin- or caveolae-related endocytosis, the latter known to play an important role in EC function, including regulation of eNOS/NO production, redox status as well as Ca^{2+} homeostasis (Figure 6E; Table VIII in the Data Supplement).[29] Altogether, our in situ differential expression analysis identified functions and associated genes converging on several pathways that previously have been associated with regulation of EC functionality, most notably, Ca^{2+} and NO.

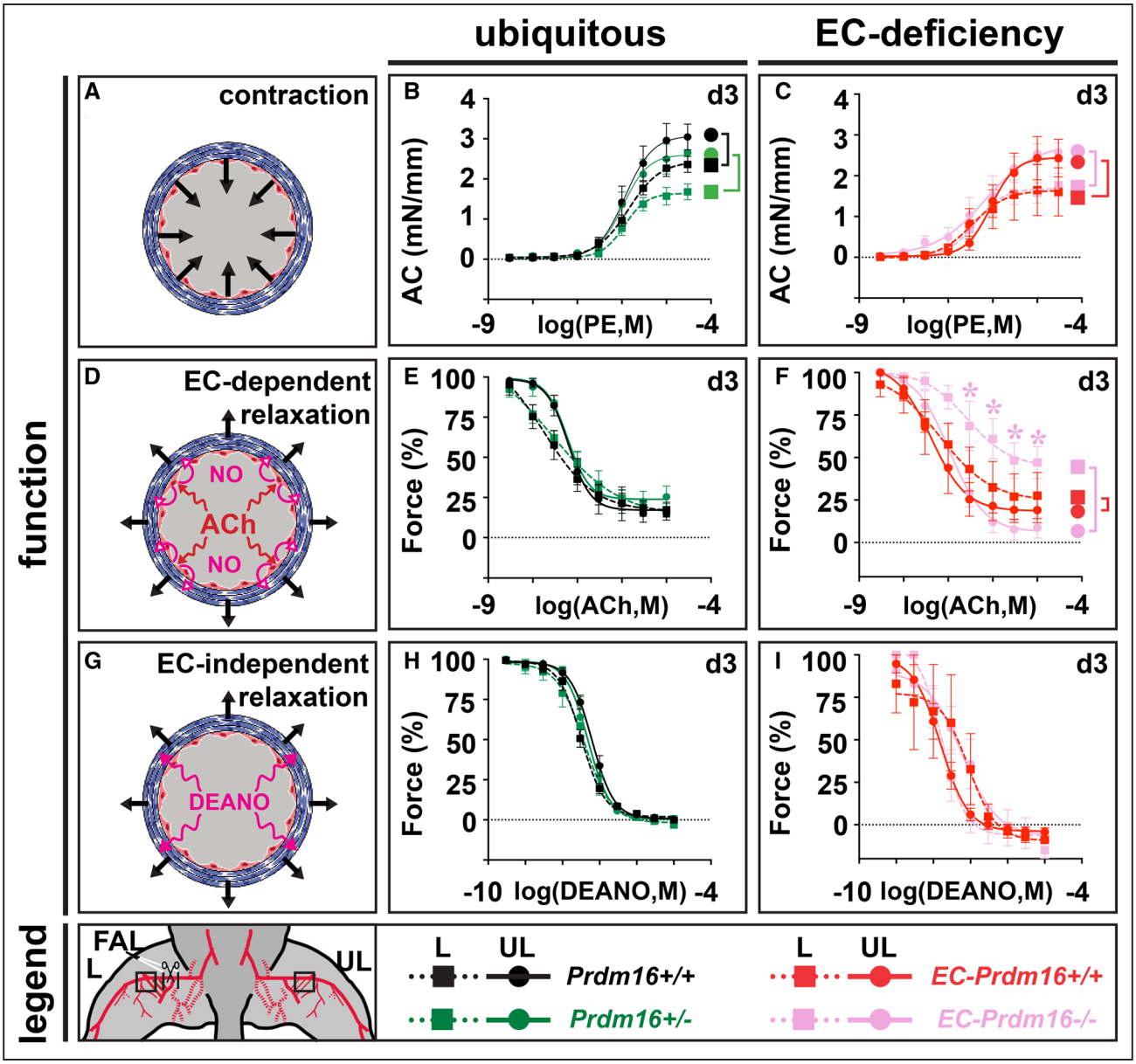

Figure 5. Endothelial cell (EC)–specific *Prdm (positive regulatory domain-containing protein) 16* deficiency causes impaired EC-dependent relaxation upon hindlimb ischemia.

A–**C**, Schematic representation (**A**) and quantification of phenylephrine (PE)-mediated absolute contraction (AC) in femoral artery (FA) segments of the ligated (L) and unligated (UL) side 3 d after FA ligation (FAL) in *Prdm16*$^{+/+}$ (n=7) or *Prdm16*$^{+/-}$ (n=5–6) mice (**B**) and long-term *EC-Prdm16*$^{+/+}$ (n=3–5) or *EC-Prdm16*$^{-/-}$ (n=4–5) mice (**C**). **D**–**F**, Schematic representation (**D**) and quantification of relative EC-dependent relaxation upon administration of acetylcholine (ACh) in FA segments at d 3 after FAL in *Prdm16*$^{+/+}$ (n=7) or *Prdm16*$^{+/-}$ (n=5–6) mice (**E**) and long-term *EC-Prdm16*$^{+/+}$ (n=3–5) or *EC-Prdm16*$^{-/-}$ (n=4–5) mice (**F**). **G**–**I**, Schematic representation (**G**) and quantification of relative EC-independent relaxation upon administration of diethylamine NONOate (DEANO) in FA segments at d 3 after FAL in *Prdm16*$^{+/+}$ (n=7) or *Prdm16*$^{+/-}$ (n=5–6) mice (**H**) and long-term *EC-Prdm16*$^{+/+}$ (n=3–5) or *EC-Prdm16*$^{-/-}$ (n=4–5) mice (**I**). Data represent mean±SEM. *P<0.05: vs indicated condition (significance is only indicated in case of a differential genotypic response to FAL; Table III in the Data Supplement). M in (B, C, E, F, H, I) indicates molar.

To verify a role for endothelial Prdm16 in Ca^{2+} and NO homeostasis upon HLI, we performed additional experiments. Given the technical complexity of in vivo Ca^{2+} measurements in the FA, and because ECs in culture rapidly lose Prdm16 expression,[9] we used a complementary approach based on intracellular Ca^{2+} measurements upon Prdm16 overexpression in human umbilical vein ECs. Prdm16 overexpression increased intracellular Ca^{2+} storage by ≈18% (Figure 7A) as measured by exposing cells to the ionophore ionomycin upon chelation of extracellular Ca^{2+}. Repeating these experiments using thapsigargin, which causes depletion of the ER Ca^{2+} store, instead of ionomycin, showed that this increase in stored Ca^{2+} was not at the level of

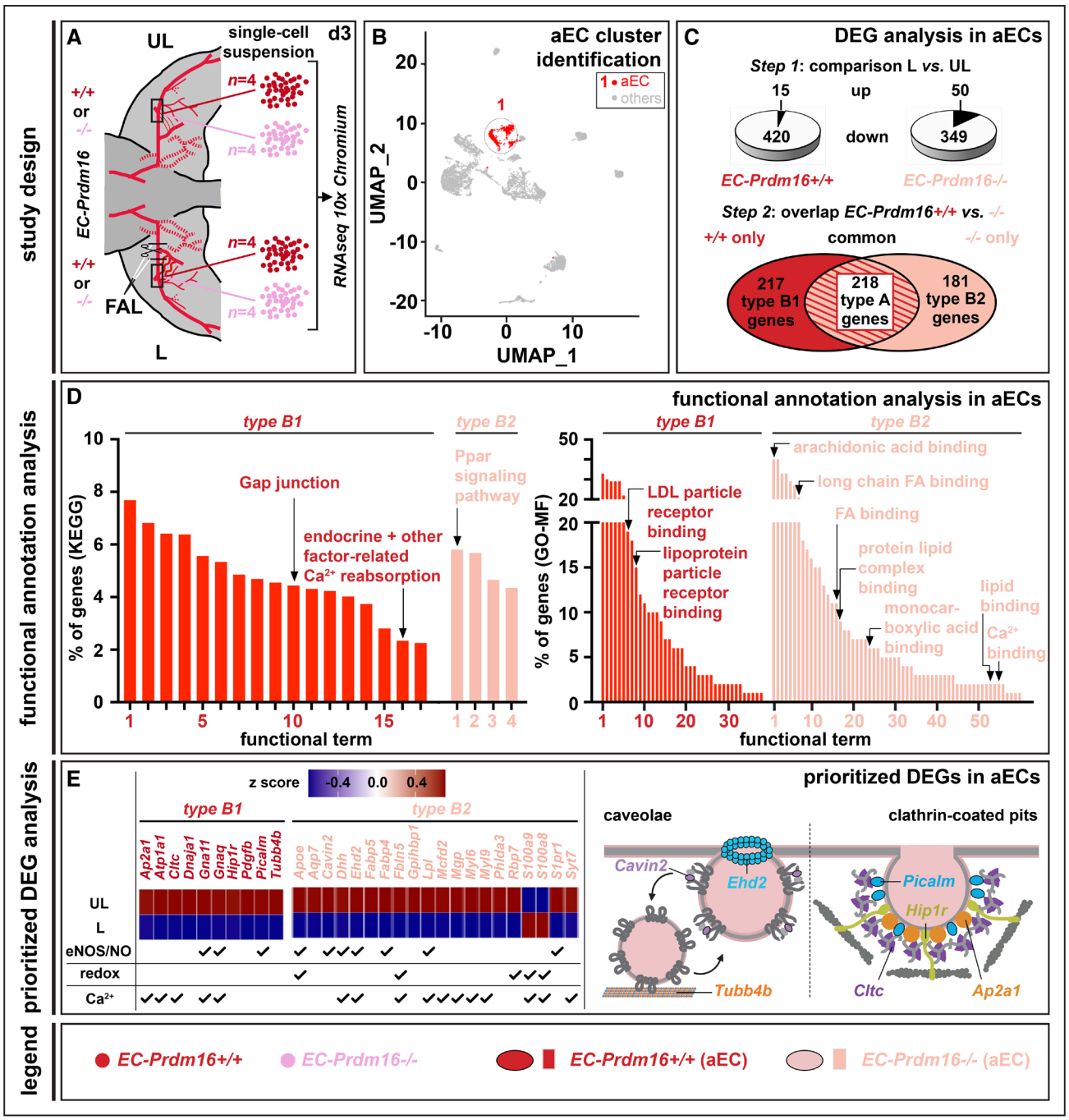

Figure 6. In situ analyses upon hindlimb ischemia induction in endothelial cell (EC)–specific *Prdm (positive regulatory domain-containing protein) 16*–deficient mice and their wild-type littermates reveal differential expression changes related to NO bioavailability and Ca^{2+} homeostasis.

A, Schematic representation of the study design for the in situ differential expression analysis based on single-cell RNA sequencing 3 d after femoral artery ligation (FAL). The regions of interest (ROI) from which single-cell suspensions from the ligated (L) or unligated (UL) side were generated for *EC-Prdm16*$^{+/+}$ (red) and *EC-Prdm16*$^{-/-}$ (dark pink) mice are indicated by a black box. The ROI material from 4 animals was pooled to obtain sufficient cells. **B**, Uniform Manifold Approximation and Projection (UMAP) plot highlighting cell clusters annotated as arterial endothelial cell (aEC) in red. **C**, Schematic representation of the 2-step model used for identification of differentially expressed genes (DEGs) in aECs that were commonly (type A; red) or genotype-dependently (type B; light pink) altered when comparing the ligated (L) vs the unligated (UL) side. **D**, Diagrams showing results of the combined functional annotation analysis by Database for Annotation, Visualization and Integrated Discovery and Gene Set Enrichment Analysis for Kyoto Encyclopedia of Genes and Genomes (KEGG; **left**) and for Gene Ontology terms molecular_functions (GO-MF; **right**), expressed as % of genes of the total number of DEGs. Functional categories prioritized because of their known association with EC (dys)function are named. **E**, Heat maps (**upper left**) showing the 30 genes represented by the prioritized functional terms in **D**. Color scale code is shown on **top**. Table (**lower left**) showing the documented involvement of the genes in regulation of eNOS (endothelial NO synthase)/NO production, redox state, and Ca^{2+} homeostasis. Cartoon (**right**) reveals location of genes encoding for structural components of caveolae or clathrin-coated pits. Arrows indicate caveolae recycling. LDL indicates low-density lipoprotein.

ORIGINAL RESEARCH

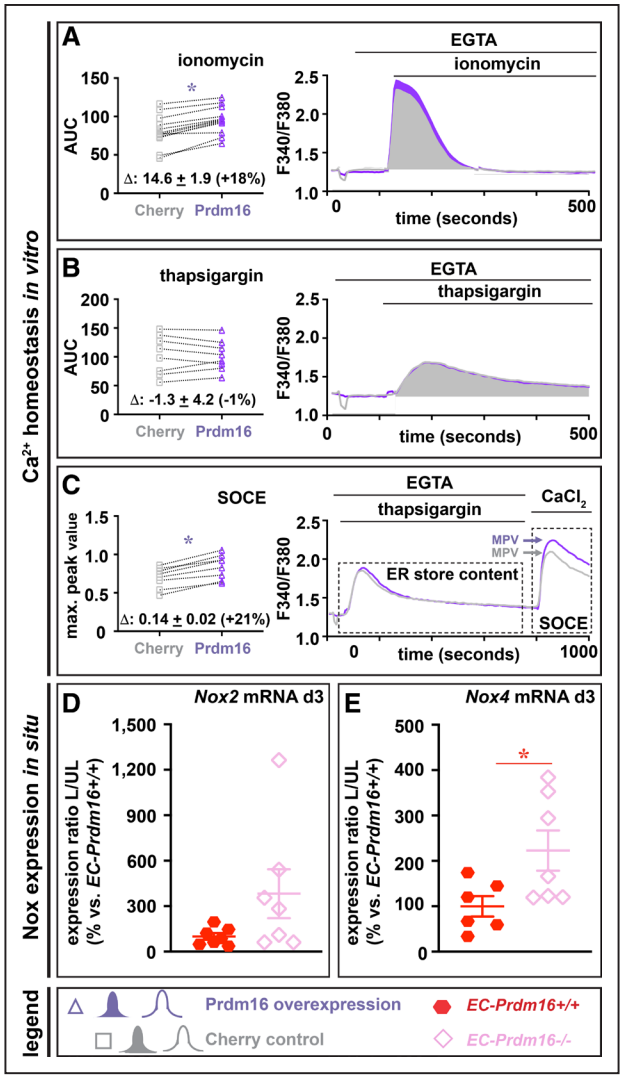

Figure 7. Prdm (positive regulatory domain-containing protein) 16 regulates Ca2+ homeostasis and *Nox* (*NADPH-oxidase*) gene expression.

A–**C**, In vitro Ca^{2+} handling experiments following treatment of Prdm16- or Cherry-overexpressing human umbilical vein endothelial cells (ECs) with ionomycin in Ca^{2+}-free medium (**A**; n=12; quantified as area under the curve [AUC]), thapsigargin in Ca^{2+}-free medium (**B**; n=8; quantified as AUC) and exposure to high extracellular Ca^{2+} following endoplasmic reticulum (ER) Ca^{2+} depletion using thapsigargin treatment as a measure for store-operated calcium entry (**C**; n=8; quantified as maximum peak value (MPV) of the response to $CaCl_2$). Mean differences between Cherry and Prdm16 overexpression conditions and corresponding % change are indicated above the X-axis in diagrams on the **left**. **D** and **E**, Diagram showing expression of *Nox2* (**D**) and *Nox4* (**E**; expressed as ratio of ligated (L) vs unligated (UL) side and as % of *EC-Prdm16*$^{+/+}$) in the adductor muscle of long-term *EC-Prdm16*$^{+/+}$ (red; n=6–7) or *EC-Prdm16*$^{-/-}$ (pink; n=7) mice at 3 d postligation. Data represent mean±SEM. *P<0.05 vs indicated condition (Table III in the Data Supplement). EGTA indicates ethylene glycol tetraacetic acid; and SOC, store-operated Ca^{2+} entry.

the ER (Figure 7B). Finally, store-operated Ca^{2+} entry, measured by readdition of extracellular Ca^{2+} after ER depletion with thapsigargin, was increased by ≈21% upon Prdm16 overexpression (Figure 7C). To further support the involvement of Prdm16 in NO bioavailability upon HLI, we investigated the levels of eNOS and Nox in situ. Although induction of eNOS protein expression in the adductor region was not affected by endothelial *Prdm16* deficiency (eNOS protein, expressed as ratio of ligated versus unligated side of *EC-Prdm16*$^{+/+}$ versus *EC-Prdm16*$^{-/-}$ mice: 1.4±0.5 versus 1.1±0.4; n=3–4, P=8.57×10^{-1} by Mann-Whitney test; Figure X in the Data Supplement), induction of *Nox2* and *Nox4* expression was increased in *EC-Prdm16*$^{-/-}$ mice suggesting more eNOS uncoupling (Figure 7D and 7E). Altogether, these findings suggest that Prdm16 controls EC function by affecting Ca^{2+} signaling and NO availability.

DISCUSSION

Currently, there are no effective options to restore arterial flow in PAD patients ineligible for invasive revascularization.[4,5] The lack of specificity towards the arterial part of the vasculature may be one reason for the inefficacy of VEGF- or FGF-based angiogenic growth factor monotherapy.[30] Identifying transcriptional regulators orchestrating arterial flow recovery may lead to development of more tailored strategies. Here, we report that loss of the arterial-restricted transcription factor Prdm16 significantly impaired flow recovery in a mouse PAD model. Intriguingly, *Prdm16* deficiency did not compromise the arterial remodeling response that classically occurs in this model, but its absence in ECs significantly attenuated EC-dependent relaxation upon HLI induction. Our unbiased screen for molecular targets downstream of Prdm16 unveiled a potential role in regulating NO bioavailability and Ca^{2+} homeostasis.

Apart from its expression in mouse retinal arterioles,[17] this transcription factor has not been reported in adult blood vessels nor was its role known in this compartment. Here, we performed a systematic analysis of Prdm16 expression in adult blood vessels and found it to be universally restricted to arteri(ol)es, independent of artery type, location, caliber, or health status. Due to this arterial-specific expression, we hypothesized a crucial role for Prdm16 during adaptive arteriogenesis. Arterial flow recovery was severely impaired, even when only one *Prdm16*-allele was missing. Unexpectedly, this impairment caused by *Prdm16* deficiency was not due to an attenuated arterial remodeling response, unlike we previously reported for Msx1.[7] The increased angiogenic response in the gastrocnemius muscle of *Prdm16*$^{+/-}$ mice likely represented an insufficient compensatory attempt to improve blood distribution in this area. In contrast to Msx1,[7] Prdm16 expression was not triggered by shear stress or hypoxia in vitro (not shown) nor in vivo, which is in line with our current observation that Prdm16 is not directly involved in driving the shear stress-induced collateral remodeling or the hypoxia-induced angiogenic response in the adductor and

gastrocnemius region, respectively. Rather, Prdm16 has an early role in arterial flow recovery by preservation of endothelial function. This not only demonstrates that the mechanism by which arterial transcription factors affect arterial flow recovery can be fundamentally different but it also suggests that proper collateral remodeling and the angiogenic response alone are not sufficient for full arterial flow restoration. Our findings are in line with a previous study in mice with a heterozygous deficiency for Notch ligand *Delta-like ligand 4* (*Dll4*) from which the authors concluded that ischemic recovery is not simply determined by the extent of the collateral network but rather by normal vascular function.[31] Although it remains to be determined whether adaptive arteriogenesis also encompasses changes in arterial specification, this process is likely more important during development than in adult, as previously reported in the same study.[31]

The flow recovery deficit upon *Prdm16* deficiency resulted in fibrosis, fibro-adipose tissue accumulation, and toe loss. Although these could be manifestations indirectly caused by lack of oxygen supply, they may also result from a direct effect of *Prdm16* deficiency. Quantitative real-time polymerase chain reaction analysis of gastrocnemius tissue at day 3 postligation revealed that endothelial *Prdm16* deficiency tended to alter expression of genes encoding fibrosis regulators (not shown), some of which (ie, tissue inhibitor of metalloproteinases (*Timp*)*1* and *Timp4*) were altered in the same way in our single-cell RNA sequencing dataset (Table V in the Data Supplement), suggesting those genes may be directly targeted by Prdm16. However, fibro-adipose tissue accumulation in *Prdm16*$^{+/-}$ gastrocnemius muscles was likely not resulting from a direct effect of Prdm16 on adipogenic differentiation of mesenchymal precursors since lack of *Prdm16* in the latter is known to decrease adipogenesis.[12] The fact that we found a similar increase in fibro-adipose tissue upon loss of *Prdm16* in nonmesenchymal cells, that is, ECs, further argues against this direct effect scenario. Finally, the increased occurrence of toe loss upon endothelial *Prdm16* deficiency may potentially be related to neuropathy, as the latter has been associated with EC dysfunction through breakdown of the peripheral blood-nerve barrier.[32]

In search of the cell type(s) responsible for the flow recovery deficit, we used cell type–specific knockout mice. Although EC-specific loss of *Prdm16* recapitulated—and even somewhat aggravated—the reperfusion deficit observed in *Prdm16*$^{+/-}$ mice, *Prdm16* loss in SMCs did not. This suggests that Prdm16 expression in ECs had a dominant role in guaranteeing normal arterial flow recovery after FA ligation. Although this precludes an important role for SMC-Prdm16 in the current PAD model, our findings do not exclude its potential importance in other (arterial) disease models. Like in *Prdm16*$^{+/-}$ mice, mice completely lacking Prdm16 in their ECs had a normal collateral growth response. However, *EC-Prdm16*$^{-/-}$ mice showed significantly attenuated EC-dependent vasorelaxation of the FA segment connecting downstream of the ligation with the collateral network but not in the upstream DA or the contralateral unligated FA segments. This indicates that the dysfunction was specifically unveiled in the region affected by the pathological challenge and that proper EC function is a critical determinant of normal arterial flow recovery, in line with the previous findings in *Dll4*$^{+/-}$ mice.[31] To our knowledge, this is the first report of vasomotor function recordings in a PAD model. Our recordings did not only reveal a defective response in *EC-Prdm16*$^{-/-}$ mice compared with their WT littermates but also showed that HLI per se caused the FA to become less capable of responding.

Although *Prdm16*$^{+/-}$ and *EC-Prdm16*$^{-/-}$ mice both had impaired flow recovery, EC-dependent relaxation was only affected in the latter. This could be explained in different ways. First, there may be gene dose-dependency, such that abnormal vasomotor responses are only present upon homozygous lack of *Prdm16* in ECs. Second, as mentioned above, *Prdm16* deficiency in non-ECs may also contribute to the flow recovery deficit in *Prdm16*$^{+/-}$ mice. Third, *Prdm16* deficiency in ECs may encompass other features of EC dysfunction not revealed by the used set of vasomotor tests. When looking in more detail at our vasomotor recordings, we noticed that contraction-relaxation curves of the ligated FA segments of 80% of *Prdm16*$^{+/-}$ (Figure XI in the Data Supplement) and 75% of *EC-Prdm16*$^{-/-}$ mice featured spikes, suggestive for abnormal vascular function. A broader interference with EC homeostasis is also supported by our unbiased screen for molecular mechanisms that could account for a Prdm16-related role in preserving EC function.

We performed this unbiased screen by an in situ differential expression analysis at single-cell resolution in arterial ECs. The Prdm16-dependent functions and associated genes emerging from this analysis converged on a broad role for Prdm16 in processes previously associated with many aspects of EC (dys)function, including regulation of eNOS production/activation, redox and Ca^{2+} homeostasis, gap junctions, and fat(ty)acid handling.[29,33–35] Indeed, endothelial *Prdm16*-deficiency affected the in situ expression of several genes previously associated with eNOS activation, including *Cavin2* and EH domain-containing (*Ehd*)*2*.[36,37] Furthermore, a role for Prdm16 in promoting NO bioavailability during HLI was supported by the fact that endothelial loss of *Prdm16* upregulated *Nox* genes, known to cause eNOS uncoupling and oxidative stress[29] and downregulated several genes that protect against oxidative stress (eg, fibulin [*Fbln*]*5* and retinol-binding protein [*Rbp*]*7*).[38,39] A role for Prdm16 in Ca^{2+} homeostasis also emerged from our in situ expression analysis, and we validated this by in vitro functional studies. In the PAD model used in the current study, the sudden increased perfusion in collaterals and the connecting downstream FA alters extracellular Ca^{2+} concentrations to which ECs are

exposed and the shear stress sensed by ECs triggers an intracellular Ca^{2+} response through release from internal stores.[40] Prdm16 overexpression did not seem to affect the Ca^{2+} content of the major intracellular store, that is, the ER, suggesting that other compartments, for example, mitochondria (representing the second-largest Ca^{2+} store), may be involved.[40,41] Intriguingly, endothelial Prdm16 regulated several genes encoding structural components of endocytotic organelles, that is, caveolae and clathrin-coated pits (Figure 6E; Table VIII in the Data Supplement) and clathrin-related functional terms emerged from our annotation analysis (Table VII in the Data Supplement). It is known that caveolae play an important role in EC function, including regulation of eNOS/NO production and oxidative stress through recruitment of Nox as well as in Ca^{2+} homeostasis.[29] Although clathrin-mediated endocytosis has not been associated with eNOS/NO production, several structural genes localized in clathrin-coated pits have been associated with Ca^{2+} handling (Figure 6E; Table VIII in the Data Supplement).

In conclusion, our study demonstrates an unprecedented role for Prdm16 in sustaining arterial flow recovery in a mouse PAD model, mainly by preserving endothelial function, rather than affecting structural remodeling. Our findings may have important implications for the design of future therapeutic avenues for no-option PAD patients. Inducing collateral growth or angiogenesis per se may be insufficient for recovery from an ischemic insult, but approaches aimed at collateral arterial network expansion should be complemented with those aiming at preserving arterial functionality. Our data indicate that the arterial-restricted transcription factor Prdm16 is an appealing target to design such complementary approaches.

ARTICLE INFORMATION

Received November 5, 2020; revision received March 30, 2021; accepted April 26, 2021.

Affiliations

Department of Cardiovascular Sciences, Center for Molecular and Vascular Biology (S.C., J.V.W., W.D., N.C., E.A.V.J., A.Z., M.B., A.L.), Laboratory for Translational Genetics, Department of Human Genetics (B.B., D.L.), Laboratory of Molecular and Cellular Signaling, Department of Cellular and Molecular Medicine (T.V.), Prometheus, Division of Skeletal Tissue Engineering (C.G.), and Skeletal Biology and Engineering Research Center, Department of Development and Regeneration (C.G.), KU Leuven, Leuven, Belgium. Pharmaceutical Sciences, Physiopharmacology, University of Antwerp, Antwerp, Belgium (S.D.M., D.D.M., A.J.A.L., P.F.). VIB Center for Cancer Biology, Leuven, Belgium (B.B., D.L.). Brigham and Women's Hospital, Harvard Medical School, Boston, MA, USA (M.B.).

Acknowledgments

We thank P. Vandervoort, B. Hoekman, E. Caluwé, M. Lox, T. Van Brussel, and R. Schepers for technical support and G. Bultynck for helpful discussions. The nano–computed tomography (CT) images have been generated on the X-ray CT facility of the Department of Development and Regeneration of KU Leuven, financed by the Hercules Foundation (project AKUL/13/47). The computational resources and services related to single-cell RNA sequencing were provided by the VSC (Vlaams Supercomputer Centrum), funded by the Fonds voor Wetenschappelijk Onderzoek (FWO), and the Flemish Government–Department Economie, Wetenschap en Innovatie (EWI).

Sources of Funding

This work was supported by a European Commission Grant (FP7-StG-IMAGINED203291), research grants from Fonds voor Wetenschappelijk Onderzoek (FWO; G0B0913N, G0A2214N, G099521N to A. Luttun; and G091018N to E.A.V. Jones), a Program Financing grant (PF/10/014) to A. Luttun; KU Leuven Geconcerteerde Onderzoeksacties (GOA11/012), Interuniversity Attraction Poles (IUAP/P7/07) and KU Leuven Research Coordination (C12/16/023; C14/19/095) grants to A. Luttun, A. Zwijsen, and E.A.V. Jones; ERA-Net ([LY-MIT-DYS] funding to E.A.V. Jones; FWO Strategic Basic Research predoctoral fellowships to J. Van Wauwe (1S25817N) and D. De Munck (1S05216N); FWO predoctoral fellowships to W. Dheedene (1157318 N) and N. Criem (1127815 N); a Bijzonder Onderzoekfonds voor Geconcentreerde Onderzoeksacties grant to S. De Moudt (33931), an Agentschap voor Innovatie door Wetenschap en Technologie (IWT; SB/0881071) predoctoral fellowship to M. Beerens and an FWO postdoctoral fellowship to T. Vervliet (12H2120N).

Disclosures

None.

Supplemental Materials

Expanded Methods
Data Supplement Figures I–XI
Data Supplement Tables I–VIII
References 6,7,9,13,18–27

REFERENCES

1. Dejana E, Hirschi KK, Simons M. The molecular basis of endothelial cell plasticity. *Nat Commun.* 2017;8:14361. doi: 10.1038/ncomms14361
2. Potente M, Mäkinen T. Vascular heterogeneity and specialization in development and disease. *Nat Rev Mol Cell Biol.* 2017;18:477–494. doi: 10.1038/nrm.2017.36
3. Fowkes FG, Rudan D, Rudan I, Aboyans V, Denenberg JO, McDermott MM, Norman PE, Sampson UK, Williams LJ, Mensah GA, et al. Comparison of global estimates of prevalence and risk factors for peripheral artery disease in 2000 and 2010: a systematic review and analysis. *Lancet.* 2013;382:1329–1340. doi: 10.1016/S0140-6736(13)61249-0
4. Gupta R, Tongers J, Losordo DW. Human studies of angiogenic gene therapy. *Circ Res.* 2009;105:724–736. doi: 10.1161/CIRCRESAHA.109.200386
5. Annex BH. Therapeutic angiogenesis for critical limb ischaemia. *Nat Rev Cardiol.* 2013;10:387–396. doi: 10.1038/nrcardio.2013.70
6. Scholz D, Ziegelhoeffer T, Helisch A, Wagner S, Friedrich C, Podzuweit T, Schaper W. Contribution of arteriogenesis and angiogenesis to postocclusive hindlimb perfusion in mice. *J Mol Cell Cardiol.* 2002;34:775–787. doi: 10.1006/jmcc.2002.2013
7. Vandersmissen I, Craps S, Depypere M, Coppiello G, van Gastel N, Maes F, Carmeliet G, Schrooten J, Jones EA, Umans L, et al. Endothelial Msx1 transduces hemodynamic changes into an arteriogenic remodeling response. *J Cell Biol.* 2015;210:1239–1256. doi: 10.1083/jcb.201502003
8. Fan Y, Lu H, Liang W, Garcia-Barrio MT, Guo Y, Zhang J, Zhu T, Hao Y, Zhang J, Chen YE. Endothelial TFEB (Transcription Factor EB) positively regulates postischemic angiogenesis. *Circ Res.* 2018;122:945–957. doi: 10.1161/CIRCRESAHA.118.312672
9. Aranguren XL, Agirre X, Beerens M, Coppiello G, Uriz M, Vandersmissen I, Benkheil M, Panadero J, Aguado N, Pascual-Montano A, et al. Unraveling a novel transcription factor code determining the human arterial-specific endothelial cell signature. *Blood.* 2013;122:3982–3992. doi: 10.1182/blood-2013-02-483255
10. Chi J, Cohen P. The multifaceted roles of PRDM16: adipose biology and beyond. *Trends Endocrinol Metab.* 2016;27:11–23. doi: 10.1016/j.tem.2015.11.005
11. Mochizuki N, Shimizu S, Nagasawa T, Tanaka H, Taniwaki M, Yokota J, Morishita K. A novel gene, MEL1, mapped to 1p36.3 is highly homologous to the MDS1/EVI1 gene and is transcriptionally activated in t(1;3)(p36;q21)-positive leukemia cells. *Blood.* 2000;96:3209–3214.
12. Seale P, Bjork B, Yang W, Kajimura S, Chin S, Kuang S, Scimè A, Devarakonda S, Conroe HM, Erdjument-Bromage H, et al. PRDM16 controls a brown fat/skeletal muscle switch. *Nature.* 2008;454:961–967. doi: 10.1038/nature07182
13. Bjork BC, Turbe-Doan A, Prysak M, Herron BJ, Beier DR. Prdm16 is required for normal palatogenesis in mice. *Hum Mol Genet.* 2010;19:774–789. doi: 10.1093/hmg/ddp543

14. Aguilo F, Avagyan S, Labar A, Sevilla A, Lee DF, Kumar P, Lemischka IR, Zhou BY, Snoeck HW. Prdm16 is a physiologic regulator of hematopoietic stem cells. *Blood.* 2011;117:5057–5066. doi: 10.1182/blood-2010-08-300145
15. Chuikov S, Levi BP, Smith ML, Morrison SJ. Prdm16 promotes stem cell maintenance in multiple tissues, partly by regulating oxidative stress. *Nat Cell Biol.* 2010;12:999–1006. doi: 10.1038/ncb2101
16. Arndt AK, Schafer S, Drenckhahn JD, Sabeh MK, Plovie ER, Caliebe A, Klopocki E, Musso G, Werdich AA, Kalwa H, et al. Fine mapping of the 1p36 deletion syndrome identifies mutation of PRDM16 as a cause of cardiomyopathy. *Am J Hum Genet.* 2013;93:67–77. doi: 10.1016/j.ajhg.2013.05.015
17. Groman-Lupa S, Adewumi J, Park KU, Brzezinski JA IV. The transcription factor Prdm16 marks a single retinal Ganglion cell subtype in the mouse retina. *Invest Ophthalmol Vis Sci.* 2017;58:5421–5433. doi: 10.1167/iovs.17-22442
18. Wang Y, Nakayama M, Pitulescu ME, Schmidt TS, Bochenek ML, Sakakibara A, Adams S, Davy A, Deutsch U, Lüthi U, et al. Ephrin-B2 controls VEGF-induced angiogenesis and lymphangiogenesis. *Nature.* 2010;465:483–486. doi: 10.1038/nature09002
19. Cohen P, Levy JD, Zhang Y, Frontini A, Kolodin DP, Svensson KJ, Lo JC, Zeng X, Ye L, Khandekar MJ, et al. Ablation of PRDM16 and beige adipose causes metabolic dysfunction and a subcutaneous to visceral fat switch. *Cell.* 2014;156:304–316. doi: 10.1016/j.cell.2013.12.021
20. Holtwick R, Gotthardt M, Skryabin B, Steinmetz M, Potthast R, Zetsche B, Hammer RE, Herz J, Kuhn M. Smooth muscle-selective deletion of guanylyl cyclase-A prevents the acute but not chronic effects of ANP on blood pressure. *Proc Natl Acad Sci U S A.* 2002;99:7142–7147. doi: 10.1073/pnas.102650499
21. Leloup AJ, Van Hove CE, Kurdi A, De Moudt S, Martinet W, De Meyer GR, Schrijvers DM, De Keulenaer GW, Fransen P. A novel set-up for the ex vivo analysis of mechanical properties of mouse aortic segments stretched at physiological pressure and frequency. *J Physiol.* 2016;594:6105–6115. doi: 10.1113/JP272623
22. Meisner JK, Annex BH, Price RJ. Despite normal arteriogenic and angiogenic responses, hind limb perfusion recovery and necrotic and fibroadipose tissue clearance are impaired in matrix metalloproteinase 9-deficient mice. *J Vasc Surg.* 2015;61:1583–94.e1. doi: 10.1016/j.jvs.2014.01.038
23. De Moudt S, Leloup A, Van Hove C, De Meyer G, Fransen P. Isometric stretch alters vascular reactivity of mouse aortic segments. *Front Physiol.* 2017;8:157. doi: 10.3389/fphys.2017.00157
24. Leloup AJ, Van Hove CE, Heykers A, Schrijvers DM, De Meyer GR, Fransen P. Elastic and muscular arteries differ in structure, basal NO production and voltage-gated Ca(2+)-channels. *Front Physiol.* 2015;6:375. doi: 10.3389/fphys.2015.00375
25. Finak G, McDavid A, Yajima M, Deng J, Gersuk V, Shalek AK, Slichter CK, Miller HW, McElrath MJ, Prlic M, et al. MAST: a flexible statistical framework for assessing transcriptional changes and characterizing heterogeneity in single-cell RNA sequencing data. *Genome Biol.* 2015;16:278. doi: 10.1186/s13059-015-0844-5
26. Korsunsky I, Millard N, Fan J, Slowikowski K, Zhang F, Wei K, Baglaenko Y, Brenner M, Loh PR, Raychaudhuri S. Fast, sensitive and accurate integration of single-cell data with Harmony. *Nat Methods.* 2019;16:1289–1296. doi: 10.1038/s41592-019-0619-0
27. Stuart T, Butler A, Hoffman P, Hafemeister C, Papalexi E, Mauck WM 3rd, Hao Y, Stoeckius M, Smibert P, Satija R. Comprehensive integration of single-cell data. *Cell.* 2019;177:1888–1902.e21. doi: 10.1016/j.cell.2019.05.031
28. Scholz D, Cai WJ, Schaper W. Arteriogenesis, a new concept of vascular adaptation in occlusive disease. *Angiogenesis.* 2001;4:247–257. doi: 10.1023/a:1016094004084
29. Billaud M, Lohman AW, Johnstone SR, Biwer LA, Mutchler S, Isakson BE. Regulation of cellular communication by signaling microdomains in the blood vessel wall. *Pharmacol Rev.* 2014;66:513–569. doi: 10.1124/pr.112.007351
30. Conway EM, Carmeliet P. The diversity of endothelial cells: a challenge for therapeutic angiogenesis. *Genome Biol.* 2004;5:207. doi: 10.1186/gb-2004-5-2-207
31. Cristofaro B, Shi Y, Faria M, Suchting S, Leroyer AS, Trindade A, Duarte A, Zovein AC, Iruela-Arispe ML, Nih LR, et al. Dll4-Notch signaling determines the formation of native arterial collateral networks and arterial function in mouse ischemia models. *Development.* 2013;140:1720–1729. doi: 10.1242/dev.092304
32. Roustit M, Loader J, Deusenbery C, Baltzis D, Veves A. Endothelial dysfunction as a link between cardiovascular risk factors and peripheral neuropathy in diabetes. *J Clin Endocrinol Metab.* 2016;101:3401–3408. doi: 10.1210/jc.2016-2030
33. Chabowski DS, Cohen KE, Abu-Hatoum O, Gutterman DD, Freed JK. Crossing signals: bioactive lipids in the microvasculature. *Am J Physiol Heart Circ Physiol.* 2020;318:H1185–H1197. doi: 10.1152/ajpheart.00706.2019
34. Jackson WF. Endothelial cell Ion channel expression and function in arterioles and resistance arteries. In: Levitan I, Dopico AM, eds. *Vascular Ion Channels in Physiology and Disease*. Springer International Publishing; 2016:3–36.
35. Kameritsch P, Pogoda K, Ritter A, Münzing S, Pohl U. Gap junctional communication controls the overall endothelial calcium response to vasoactive agonists. *Cardiovasc Res.* 2012;93:508–515. doi: 10.1093/cvr/cvr345
36. Boopathy GTK, Kulkarni M, Ho SY, Boey A, Chua EWM, Barathi VA, Carney TJ, Wang X, Hong W. Cavin-2 regulates the activity and stability of endothelial nitric-oxide synthase (eNOS) in angiogenesis. *J Biol Chem.* 2017;292:17760–17776. doi: 10.1074/jbc.M117.794743
37. Matthaeus C, Lian X, Kunz S, Lehmann M, Zhong C, Bernert C, Lahmann I, Müller DN, Gollasch M, Daumke O. eNOS-NO-induced small blood vessel relaxation requires EHD2-dependent caveolae stabilization. *PLoS One.* 2019;14:e0223620. doi: 10.1371/journal.pone.0223620
38. Hu C, Keen HL, Lu KT, Liu X, Wu J, Davis DR, Ibeawuchi SC, Vogel S, Quelle FW, Sigmund CD. Retinol-binding protein 7 is an endothelium-specific PPARγ cofactor mediating an antioxidant response through adiponectin. *JCI Insight.* 2017;2:e91738. doi: 10.1172/jci.insight.91738
39. Nguyen AD, Itoh S, Jeney V, Yanagisawa H, Fujimoto M, Ushio-Fukai M, Fukai T. Fibulin-5 is a novel binding protein for extracellular superoxide dismutase. *Circ Res.* 2004;95:1067–1074. doi: 10.1161/01.RES.0000149568.85071.FB
40. Scheitlin CG, Julian JA, Shanmughapriya S, Madesh M, Tsoukias NM, Alevriadou BR. Endothelial mitochondria regulate the intracellular Ca2+ response to fluid shear stress. *Am J Physiol Cell Physiol.* 2016;310:C479–C490. doi: 10.1152/ajpcell.00171.2015
41. Kluge MA, Fetterman JL, Vita JA. Mitochondria and endothelial function. *Circ Res.* 2013;112:1171–1188. doi: 10.1161/CIRCRESAHA.111.300233